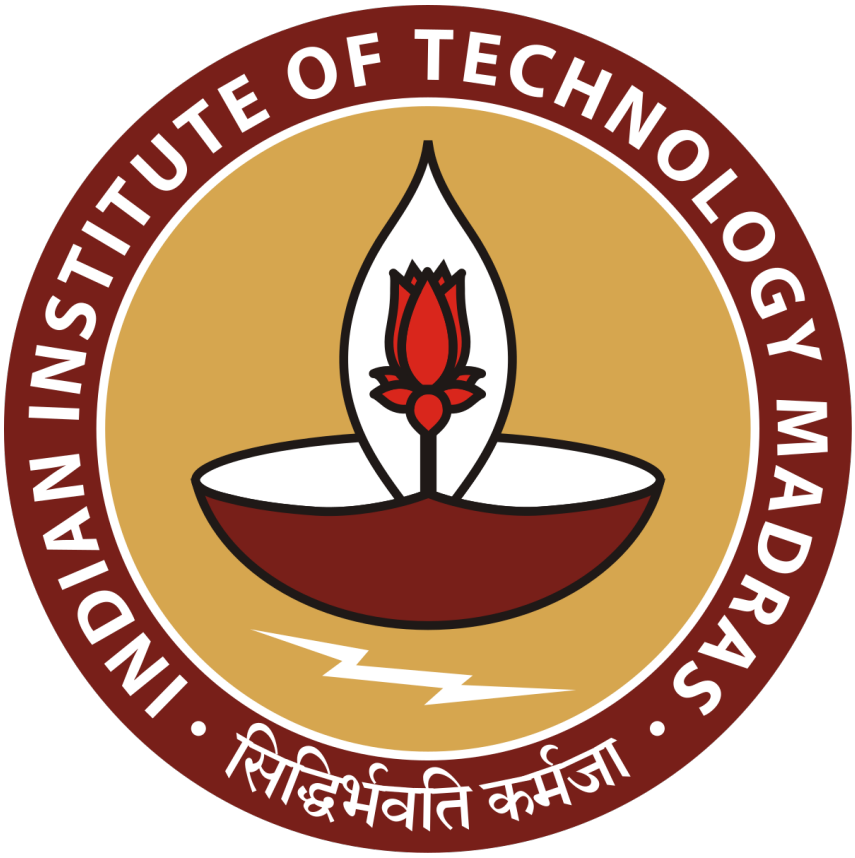

Department of Aerospace Engineering

AS5545

Dynamics and Controls of Spacecraft

A detailed report on
Satellite attitude stabilization using solar radiation pressure and magnetorquer

K.D. Kumar, M.J. Tahk, and H.C. Bang

Name: J Jeevan Roy

Roll no: AE18B029

Contents

1 Objective:

Consider passive method challenges and focus on the application of SRP and Earth's magnetic field for satellite attitude control with a view to achieve the goal of low cost ACS.

1.1 Assumptions

The Earth's magnetic field $\vec{B}$ to be a dipole and the variation in the field, considering no Earth rotation and no orbit precession, is periodic, i.e., $\vec{B}(t) = \vec{B}(t+\varphi)$, where $\varphi = 2\pi/\Omega$ denotes the orbital period. This assumption is valid for the present feasibility study because the Earth's magnetic field is asymmetric and thereby the Earth rotation and orbit precession cause only small deviations in $\vec{B}$.

Abstract The paper presents three-dimensional (3-D) attitude stabilization of a geosynchronous satellite. The SRP is considered for the satellite pitch and roll stabilization while the yaw attitude is stabilized by a magnetotorquer. The general formulation of the system comprised of a satellite body, two solar flaps, and a magnetotorquer is obtained through Euler's equations. The linearized system model is derived and then the control laws are developed for suitable rotations of solar flaps and variations in magnetic moment. The numerical simulation of the governing nonlinear system equations of motion establishes the feasibility of achieving the desired 3-D satellite attitude. The controllers are successful in stabilizing the satellite attitude even in the presence of orbital eccentricity and variations in system parameters.

2 Overview

The body of this report consists of seven main sections followed by a conclusions section. *Section 3* provides the necessary introduction. *Section 4* presents the derivation of control torques due to SRP and magnetorquers. *Section 5* presents the system model and a general formulation of the system moving in an elliptic orbit. Euler's equations are utilized to obtain the governing nonlinear equations of motion for the proposed system. In *Section 6*, the linearized system model is derived and control laws are developed for suitable rotations of solar flaps and variations in magnetic moment. Finally, for a detailed assessment of the proposed attitude control strategy, the set of governing equations of motion is numerically integrated and the effects of various parameters including the Earth's shadow on the system response are examined in *Section 9*.

3 Introduction

The attitude stability of a satellite is of considerable importance for successful completion of a space mission. The satellite's attitude experiences environmental torques due to gravity gradient, solar radiation pressure, magnetic, and free molecular reaction forces. The internal disturbances like those within the payload, e.g., sloshing of propellants, and coupling of the attitude dynamics with the orbital and flexural mechanics may also affect satellite attitude motion.

Several methods of attitude stabilization have been developed over the last four decades. These methods may be broadly classified as *active* and *passive* methods. **Active stabilization methods** require expenditure of propellant or energy, leading to an increase in weight and space requirements. Some of the well-known examples are micro-thrusters, reaction wheels, and control momentum gyros. These can control precise satellite orientation to practically any desired degree of accuracy. On the other hand, **passive stabilization methods** depend on natural forces and they make use of spin stabilization, dual spin, gravity gradient, solar radiation pressure (SRP), and Earth's magnetic field. These methods are thus low cost and their development may provide a viable solution to the recent thrust, by space researchers world- wide, on the development of low cost attitude control systems(ACS) and guidance, navigation, and control systems (GNC) for satellites. However, their development poses several challenges. **Passive Method challenges** include techniques to utilize these forces, Low attitude accuracies, and unavailability of forces.

3.1 Literature review on satellite attitude stabilization using SRP

Various configurations suggested to utilize SRP torques properly are trailing cone system, weathervane-type tail surfaces, reflector–collector system, corner mirror arrays, solar paddles, grated solar sails, and mirror-like surfaces. These concepts have been proposed for sun-pointing satellites, and gravity-oriented satellites. Spinning satellites as well as non-spinning satellites were also considered.

The attitude control of the satellite has been accomplished by translatory motions of single or several control surfaces relative to the satellite body or by rotating the control surfaces about the satellite body-fixed axes. SRP control is applied based on feedback linearization. Roll and yaw control of a geostationary satellite is examined using solar flaps.

Some missions have also been flown to verify the concept of using SRP for attitude control application. In Mariner IV mission, solar vanes in conjunction with active gyros are employed to control the spacecraft attitude along the sun-line. The European Space Agency tested viability of using SRP for attitude control of the geostationary communication satellite OTS-2. This concept is routinely used nowadays on large geostationary communications satellites. However, the potential- ities of SRP usage for attitude control remain far from realized. This, perhaps, may be attributed to the complexity of the proposed controllers and further, due to the competition with the proven conventional attitude control methods.

Note Refs:

- *Renner (1979)* and *Scull (1969)* are only papers that deal with the actual mission application of SRP control system while other references are purely academic research.
- The problem of satellite pitch attitude control is studied by *Pande* and *Venkatachalam (1981)*, *Venkatachalam (1993)*, and *Singh* and *Yim (1996)*.

- *Singh* and *Yim (1996)* applied SRP control based on feedback linearization.
- The pitch attitude control in elliptic orbits for an axisymmetric satellite is examined by *Joshi* and *Kumar (1980).*
- *Stuck (1980)* considered three-axis attitude control of a synchronous communication satellite using multiple control surfaces.
- The three-dimensional (3-D) attitude control of an axisymmetric geosynchronous satellite is studied by *Kumar (1988).*
- *Azor (1992)* examined roll and yaw control of a geosta- tionary satellite using solar flaps.

3.2 Literature review on satellite attitude stabilization using Magnetorquers

Magnetotorquers have been used for the attitude control of several satellites: Transit-1B (1960), Transit- 2A (1960), Injun-3 (1962), ESRO-1A (1968), ESRO-1B (1969), Azur (1969), Exos (1978), Magion (1978), Microsat-NA (1990), JAK (2000), Thelma (2000), Louise (2000), and Stensat (2000). They are relatively reliable, lightweight, and energy efficient. However, the magnetotorquers alone cannot guarantee global stability because of their inability to provide torque about the local magnetic field direction, for example, the pitch attitude of an equatorial orbit satellite cannot be controlled.

Investigation on this subject was first reported by White, Shigemoto, and Bourquin (1961) and thereafter, several researchers have con- tributed on this subject. The attitude control of various satellite configurations that include single-spin axisymmetric satellites, dual-spin or momentum-biased satellites, and non-spinning satellites have been examined.

Earlier research were focused mainly on the attitude control of spinning satellites using magnetotorquers. Recently, the research have shifted to only applying magnetotorquers for full three-axis attitude control of non- spinning satellites with a focus on small satellites. Particularly, in small satellites where the traditional attitude stabilization systems such as reaction wheels (momentum wheels) do not fit within the limited weight and power budget and therefore, are impractical, the magnetotorquers have been very attractive.

Open-loop control laws as well as closed-loop control laws have been proposed. In the development of the open-loop control laws, an averaging method was applied, whereas the closed-loop control laws were designed using linear and nonlinear control techniques. The linear control techniques are mostly based on linear proportional-derivative control or linear quadratic regulator (LQR) or periodic optimal control. The minimum energy is applied to develop control laws whereas the control laws are based on switching function derived from the asymptotic stability condition. Nonlinear control techniques include Lyapunov-based control, sliding mode control, model-based predictive control, and pseudospectral control.

Note Refs: The combination of SRP and magnetic torquer was considered by *Modi* and *Pande (1974a)*. In this investigation, the authors assumed an axisymmetric dual spin satellite in near-synchronous altitudes and the Earth's magnetic field was used for nutation damping while the pitch motion was controlled by SRP.

3.3 Contributions to the SRP Stabilized Satellites

The satellite pitch and roll attitudes are stabilized by rotating a pair of flaps using respective motors about two satellite-body axes instead of one-axis or instead of using several pairs of flaps (see Fig. 1). The yaw attitude is controlled by a magnetotorquer. Various uncertainties in the system parameters have been considered and the proposed controller performance is tested in the presence of these uncertainties.

3.4 system

The proposed system comprises a satellite with a pair of solar flaps, along its yaw-axis, and a magnetotorquer (Fig. 1). The solar flaps are used to control the satellite pitch and roll motions while the magnetotorquer controls satellite yaw motion.

3.5 Uncertainities

Two solar flaps may not be symmetrical. The moments of inertia of the system may differ from the designed exact inertia and the products of inertia might not be exactly zero. The orbital eccentricity may not be zero. In the solar pressure model, ρ_s may not be one ($\rho_s \neq 1$). These uncertainties can easily destabilize the system which was otherwise stable.

4 Derivation of control torques due to SRP and magnetorquers

4.1 The solar radiation force

The solar radiation force acting on a flat solar plate-j is given by

$$\vec{F}_{sj} = pA_j|\vec{s}.\vec{n}_j|\{(1-\rho_s)\vec{s} + [2\rho s(\vec{s}.\vec{n}_j) + (2/3)\rho_d]\vec{n}_j\} \tag{1}$$

where

$$\rho_s + \rho_a + \rho_d = 1 \tag{2}$$

Assuming the Sun is fixed in inertial space, $\vec{s}$, a unit vector of the incoming light from the sun on the solar flap-j, j = 1,2, is obtained in the satellite body-fixed reference frame, S-XYZ, as

$$\vec{s} = s_x\hat{i} + s_y\hat{j} + s_z\hat{k} \tag{3}$$

where

$$\begin{aligned}
s_x &= sin\,\psi\, sin(i-\epsilon_s)\, cos\,\phi\, cos\,\gamma - cos\,\psi[cos(\theta+\alpha)\, sin\,\phi\, cos\,\gamma + sin(\theta+\alpha) sin\,\gamma] \\
s_y &= -sin\,\psi\, sin(i-\epsilon_s) sin\,\phi - cos\,\psi cos(\theta+\alpha) cos\,\phi - sin\,\psi\, cos(i-\epsilon_s)\, sin(\theta+\alpha) cos\,\phi \\
s_z &= sin\,\psi\, sin\,(i-\epsilon_s)\, cos\,\phi\, sin\,\gamma - cos\,\psi[cos(\theta+\alpha)\, sin\,\phi\, sin\,\gamma - sin(\theta+\alpha) cos\,\gamma]
\end{aligned}$$

$$-sin\,\psi\,cos(i-\epsilon_s)[sin(\theta+\alpha)\,sin\,\phi\,sin\,\gamma+cos(\theta+\alpha])cos\,\gamma]$$

The vector $\vec{n_j}$ is derived as

$$\vec{n}_j = [sin\,\eta_j]\hat{i} + [-cos\,\eta_j\,sin\,\beta_j]\hat{j} + [cos\,\eta_j\,cos\,\beta_j]\hat{k} \tag{4}$$

Thus, the torque exerted by the solar flap-j on the satellite attitude is given by

$$\begin{aligned}
\vec{T}_{sj} &= \vec{r}\times\vec{F}_{sj} &(5)\\
&= r_j\hat{j}\times\vec{F}_{sj} &(6)\\
&= (-1)^{j+1}pA_jr_j|\vec{s}.\vec{n}_j|\times(\{(1-\rho_s)s_z+[2\rho_s(\vec{s}.\vec{n}_j)+(2/3)\rho_d](cos\,\eta_j cos\beta_j+)\}\hat{i}\\
&\quad -\{(1-\rho_s)s_x+[2\rho_s(\vec{s}.\vec{n}_j)+(2/3)\rho_d](sin\,\eta_j)\}\hat{k}) &(7)
\end{aligned}$$

4.2 SRP torque: The Dimensionless Torque Components

The resultant dimensionless components of the total SRP torque about the satellite body axes can be written as

$$\begin{aligned}
\hat{T}_{sx} &= C(|\vec{s}.\vec{n}_1|\,\{[(1-\rho_s)/(2\rho_s)]s_z+[(\vec{s}.\vec{n}_1)+(1/3)(\rho_d/\rho_s)]cos\,\eta_1\,cos\,\beta_1\}\\
&\quad -(1+\Delta d)|\vec{s}.\vec{n}_2|\,\{[(1-\rho_s)/(2\rho_s)]s_z+[(\vec{s}.\vec{n}_2)+(1/3)(\rho_d/\rho_s)]cos\,\eta_2\,cos\,\beta_2\}) &(8)\\
\hat{T}_{sy} &= 0 &(9)\\
\hat{T}_{sz} &= -C(|\vec{s}.\vec{n}_1|\,\{[(1-\rho_s)/(2\rho_s)]s_x+[(\vec{s}.\vec{n}_1)+(1/3)(\rho_d/\rho_s)]\,sin\,\eta_1\}\\
&\quad -(1+\Delta d)|\vec{s}.\vec{n}_2|\{[(1-\rho_s)/(2\rho_s)]s_x+[(\vec{s}.\vec{n}_2)+(1/3)(\rho_d/\rho_s)]\,sin\,\eta_2\}) &(10)
\end{aligned}$$

where

$$C = 2\rho_s pA_1r_1/(I_x\Omega^2)$$

$$and$$

$$\Delta d = (A_2r_2 - A_1r_1)/(A_1r_1).$$

The term Δd signifies error in the SRP distributions on the two solar flaps. This error might occur due to asymmetry in the solar flap areas and centers of solar radiation pressures.

4.3 Magnetic torque

The magnetic torque exerted on a satellite carrying a magnetic rod is given by

$$\vec{T}_m = \vec{M}\times\vec{B} \tag{11}$$

Assuming no Earth rotation and no orbit precession, $\vec{B}$ is obtained as

$$\vec{B} = \frac{\mu_f}{R^3}[(cos\,i_m)\hat{i}_0 - (2\,sin\,\theta\,sin\,i_m)\hat{j}_0 + (cos\,\theta\,sin\,i_m)\hat{k}_0] \tag{12}$$

along the orbital reference frame $\hat{i}_0\hat{j}_0\hat{k}_0$.

The magnetic moment of the magnetic rod, $\vec{M}$, is expressed as

$$\vec{M} = N_c I_c A_c \vec{n}_c \tag{13}$$

where $\vec{n}_c$ = unit vector normal to the coil area.

Considering the satellite in an equatorial orbit (assuming $i_m \approx 0$), $\vec{B}$ from 23 can be rewritten as

$$\vec{B} = B\hat{i}_0 \tag{14}$$

where

$$B = \mu_f / R^3$$

In terms of the satellite body-fixed reference frame, $\vec{B}$ can be written as

$$\vec{B} = B_x\hat{i} + B_y\hat{j} + B_z\hat{k} \tag{15}$$

where

$$\begin{aligned} B_x &= B\,cos\,\phi\,cos\,\gamma, \\ B_y &= -B\,sin\,\phi, \\ B_z &= B\,cos\,\phi\,sin\,\gamma. \end{aligned}$$

As the components of $\vec{M}$, that are perpendicular to $\vec{B}$ only contribute to the torque exerted on satellite, $\vec{M}$ is taken as

$$\vec{M} = \frac{\vec{\tilde{M}} \times \vec{B}}{|\vec{B}|} \tag{16}$$

Substituting the above expression for $\vec{M}$ in 11, the components of magnetic torque about the satellite body-axes are obtained as

$$T_{mx} = (1/B)[-(B_y^2 + B_z^2)\tilde{M}_x + B_x B_y \tilde{M}_y + B_x B_z \tilde{M}_z] \tag{17}$$

$$T_{my} = (1/B)[B_x B_y \tilde{M}_x - (B_x^2 + B_z^2)\tilde{M}_y + B_y B_z \tilde{M}_z] \tag{18}$$

$$T_{mz} = (1/B)[B_x B_z \tilde{M}_x + B_y B_z \tilde{M}_y - (B_x^2 + B_y^2)\tilde{M}_z] \tag{19}$$

4.4 Magnetorquer: The Dimensionless Torque Components

Since it is required to control only the yaw motion of the satellite using the magnetorquer, $\vec{M}$ is considered while $\tilde{M}_x = \tilde{M}_z = 0$. The dimensionless torque components, obtained by taking $\hat{T}_{mk} = T_{mk}/(I_x\Omega^2)$, k = x,y,z, are

$$\hat{T}_{mx} = -D_3 \tilde{M}_y\,sin\,\phi\,cos\,\phi\,cos\,\gamma \tag{20}$$

$$\hat{T}_{my} = -D_3\,\tilde{M}_y\,cos^2\,\phi \tag{21}$$

$$\hat{T}_{mz} = -D_3\,\tilde{M}_y\,sin\,\phi\,cos\,\phi\,sin\,\gamma \tag{22}$$

where

$$D_3 = \mu_f/(GM_E I_x).$$

5 System Model and Equations of Motion

The system model comprises a satellite with two-oppositely placed light-weight solar flaps along the satellite Y-axis and a magnetotorquer (Fig. 1). The system center of mass S lies on the center of mass of the satellite. The coordinate frame $X_oY_oZ_o$ passing through the satellite center of mass S represents the orbital reference frame. The nodal line represents the reference line in orbit for the measurement of the true anomaly θ (eccentric orbit) or angle θ (circular orbit). The X_o-axis is taken along normal to the orbital plane, the Y_o-axis points along the local vertical and the Z_o-axis represents the third axis of this right handed frame taken. **The orientation of the satellite** is specified by a set of three successive rotations: α (pitch) about the X_o-axis, ϕ about the new roll axis (Z_1-axis) and finally γ about the resulting yaw axis (Y_2-axis). The corresponding principal body-fixed coordinate axes of the satellite are denoted by S-XYZ. For solar flap-j, its axis considered initially aligned to the Y-axis is rotated by an angle β_j about the X-axis, followed by η_j rotation about the new Y-axis. The system under consideration has satellite rotations: pitch(α), roll(ϕ) and yaw(γ) as independent coordinates or degrees of freedom of the system.

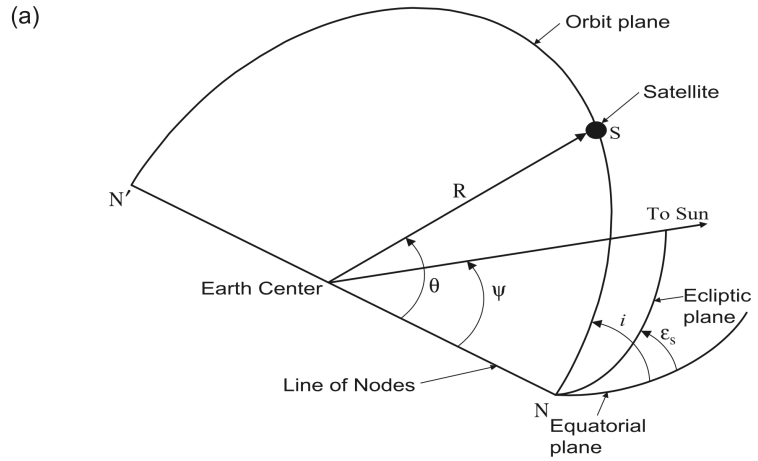

Fig. 1. (a) Geometry of orbit motion of the system.

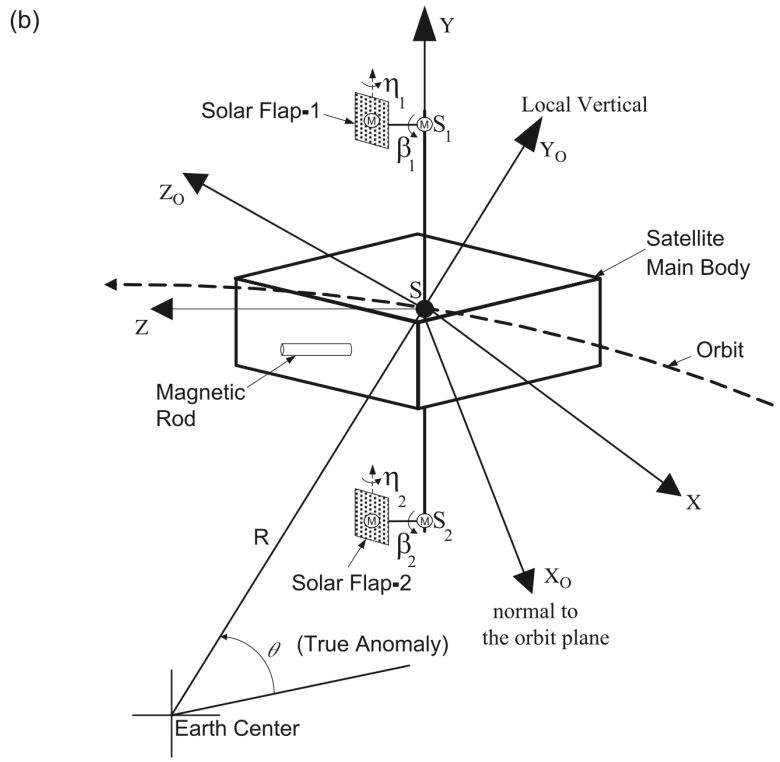

Fig. 2. (b) Geometry of the proposed controller configuration.

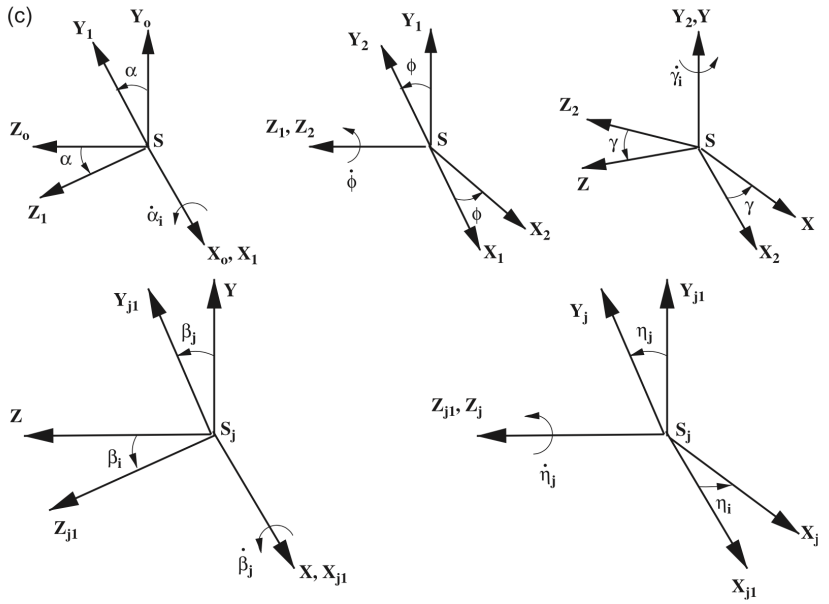

Fig. 3. (c) Orientation of the satellite and solar flap fixed coordinate frames with respect to the orbital fixed frame.

Applying Euler's moment equations the governing nonlinear coupled ordinary differential equations of motion of the system are obtained as

$$\boldsymbol{I}_S\dot{\boldsymbol{\omega}}_S + \boldsymbol{\omega}_S^{\times}\boldsymbol{I}_S\boldsymbol{\omega}_S = 3\left(\frac{\mu}{R^3}\right)\boldsymbol{C}_S^{\times}\boldsymbol{I}_S\boldsymbol{C}_S + \boldsymbol{T}_e \tag{23}$$

where

$$\boldsymbol{I}_S = \begin{pmatrix} I_{XX} & -I_{XY} & -I_{XZ} \\ -I_{YX} & I_{YY} & -I_{YZ} \\ -I_{ZX} & -I_{ZY} & I_{ZZ} \end{pmatrix},$$

$$\boldsymbol{\omega}_S = \begin{bmatrix} \omega_X \\ \omega_Y \\ \omega_Z \end{bmatrix} = \begin{bmatrix} (\dot{\theta}+\dot{\alpha})cos\phi cos\gamma - \dot{\phi}sin\gamma \\ -(\dot{\theta}+\dot{\alpha})sin\phi + \dot{\gamma} \\ (\dot{\theta}+\dot{\alpha})cos\phi sin\gamma + \dot{\phi}cos\gamma \end{bmatrix},$$

$$\boldsymbol{\omega}_S^{\times} = \begin{pmatrix} 0 & -\omega_Z & \omega_Y \\ \omega_Z & 0 & \omega_X \\ -\omega_Y & -\omega_X & 0 \end{pmatrix},$$

$$\boldsymbol{C}_S = \begin{bmatrix} C_X \\ C_Y \\ C_Z \end{bmatrix} = \begin{bmatrix} cos\alpha\, sin\phi\, cos\gamma + sin\alpha\, sin\gamma \\ cos\alpha\, cos\gamma \\ cos\alpha\, sin\phi\, sin\gamma\ - sin\alpha\, cos\gamma \end{bmatrix},$$

The $\boldsymbol{T}_e$ in Eq. (1) is an external torque vector acting on the spacecraft due to the SRP torque, T_{sk}, k = x,y,z, and the magnetorquer, T_{mk}, k = x,y,z, given as

$$\boldsymbol{T}_e = \begin{bmatrix} T_{sx} + T_{mx} \\ T_{sy} + T_{my} \\ T_{sz} + T_{mz} \end{bmatrix} \tag{24}$$

For a specified orbit, the orbital radius R and the orbital rate $\dot{\theta}$ are obtained by

$$R = \frac{p}{1 + e\,cos\,\theta} \tag{25}$$

$$\dot{\theta} = \frac{h}{R^2} \tag{26}$$

where p is the semi-latus rectum and $h = \sqrt{GM_E p}$ is the angular momentum per unit mass.

The true anomaly $\theta(t)$ is known implicitly from Kepler's equation. It is convenient to replace t by θ as the independent variable and to denote derivatives with respect to θ by primes using the following relations:

$$\dot{\boldsymbol{q}} = \dot{\theta}\boldsymbol{q}' \tag{27}$$

$$= \frac{h}{R^2}\boldsymbol{q}' \tag{28}$$

$$\ddot{\boldsymbol{q}} = \frac{GM_E}{R^3}\{(1 + e\,cos\,q)\boldsymbol{q}'' - (2\,e\,sin\,q)\boldsymbol{q}'\} \tag{29}$$

Where $\boldsymbol{q}$ is the independent system coordinate vector given as $\boldsymbol{q} = [\,\alpha\,\gamma\,\phi\,]^T$.

5.1 The Governing Equations of Motion(in Matrix Notation)

The governing equations of motion (also called as system pitch equation of motion) after carrying out algebraic manipulation and nondimensionalization are written in matrix notations as

$$M(\boldsymbol{q},\, \theta,\, e,\, \boldsymbol{I}_s)\boldsymbol{q}'' + F(\boldsymbol{q},\, \boldsymbol{q}',\, \theta,\, e,\, \boldsymbol{I}_s) = \hat{\boldsymbol{T}}_q \tag{30}$$

where M is the mass matrix and F is the vector containing all the nonlinear terms including the Coriolis and centrifugal contributions. The dimensionless external torque $\hat{\boldsymbol{T}}_q$ is given by

$$\begin{aligned} \hat{\boldsymbol{T}}_q &= \left(\frac{1-e^2}{1+e\,cos\,\theta}\right)^3 \left(\frac{\boldsymbol{T}_e}{I_x\Omega^2}\right), && (31)\\ &= \left(\frac{1-e^2}{1+e\,cos\,\theta}\right)^3 \begin{bmatrix} \hat{T}_{sx}+\hat{T}_{mx} \\ \hat{T}_{sy}+\hat{T}_{my} \\ \hat{T}_{sz}+\hat{T}_{mz} \end{bmatrix}, && (32)\\ q &= \alpha,\, \phi,\, \gamma && (33) \end{aligned}$$

where

$$\begin{aligned} \hat{T}_{sk} &= T_{sk}/(I_x\Omega^2), && (34)\\ \hat{T}_{mk} &= T_{mk}/(I_x\Omega^2), && (35)\\ k &= x, y, z. && (36) \end{aligned}$$

6 Linear System Model and Control Laws

6.1 Objective

To understand the system dynamics and thereby develop suitable control laws.

6.1.1 Assumptions

1. Small amplitude liberations.
2. Orbital eccentricity e ≈ 0.
3. Ignoring the second and higher order terms in α, ϕ, and γ.

6.2 Procedure

The complex nonlinear and nonautonomous system equations of motion given by Eq 30 and torque relations as per Eqs, 8–10 and 20–22 are simplified.

6.2.1 The resulting equations of motion of the given system

Satellite: Pitch (α)

$$\hat{T}_{sx} = \alpha'' - 3(K_{yx} - K_{zx})\alpha \tag{37}$$

Satellite: roll (ϕ)

$$\hat{T}_{sz} = K_{zx}\,\phi'' + (-1 + K_{yx} + K_{zx})\gamma' + 4(1 - K_{yx})\phi \tag{38}$$

Satellite: yaw (γ)

$$\hat{T}_{my} = K_{yx}\gamma'' + (1 - K_{yx} - K_{zx})\phi' + (1 - K_{zx})\gamma \tag{39}$$

where

$$\hat{T}_{my} = -D_3\tilde{M}_y \tag{40}$$

6.2.2 Some more Assumptions

1. A highly reflective surface of solar flap(i.e., $\rho_s \approx 1$; specular reflection only).
2. The two solar flaps are symmetrical (i.e., $A_2 r_2 \approx A_1 r_1, \Delta d \approx 0$)

6.2.3 Modified SRP torque

The SRP torque $\hat{T}_{sx}$ and $\hat{T}_{sz}$ can be expressed as

$$\begin{aligned} \hat{T}_{sx} &= 2C\,|D_1|\,[-(\eta_1 - \eta_2)sin\,\psi\,sin\,(i - \epsilon_s) + D_2\,(\beta_1 - \beta_2)] && (41)\\ \hat{T}_{sz} &= C\,|D_1|\,(\eta_1 - \eta_2) && (42) \end{aligned}$$

where

$$\begin{aligned} D_1 &= cos\,\psi\,sin\,\theta - sin\,\psi\,cos\,(i - \epsilon_s)\,cos\,\theta && (43)\\ D_2 &= cos\,\psi\,cos\,\theta + sin\,\psi\,cos\,(i - \epsilon_s)\,sin\,\theta && (44) \end{aligned}$$

Furthermore knowing that the term $-(\eta_1 - \eta_2)\,sin\,psi\,sin\,(i - \epsilon_s) << D_2(\beta_1 - \beta_2)$, the preceding relations simplified to

$$\begin{aligned} \hat{T}_{sx} &= 2C\,|D_1|\,D_2\,(\beta_1 - \beta_2) && (45)\\ \hat{T}_{sz} &= 2C\,|D_1|\,D_2(\eta_1 - \eta_2) && (46) \end{aligned}$$

6.2.4 The control Laws

Using Eqs. 37–40 and Eqs. 45 and 46, the proportional and derivative type control laws for suitable variations of control inputs: β_j, η_j, $j = 1, 2$, and $\tilde{M}_y$, can be expressed as

$$\begin{aligned} \beta_j &= (-1)^j\,sgn(D_2)\,[\mu_1\,\alpha' + \nu_1\,\alpha],\ j = 1, 2 && (47)\\ \eta_j &= (-1)^{j+1}\,sgn(D_1)\,[\mu_3\,\phi' + \nu_3\,\varphi]\,j = 1, 2 && (48)\\ \tilde{M}_y &= \mu_2\,\gamma' + \nu_2\,\gamma && (49) \end{aligned}$$

In order to prove that the preceding control laws, Eqs. 47–49 lead to the asymptotic stability of the closed-loop system, Eqs. 37–39, the Lyapunov direct method is applied.

6.2.5 Lyapunov function for the system

The Lyapunov function for the system is assumed as

$$V(X) = \frac{1}{2} P^T X P \tag{50}$$

with $V(X = 0) = 0$. Here $X = [\alpha,\, \alpha',\, \phi,\, \phi',\, \gamma,\, \gamma']^T$ and $P = diag(P_1,\, P_2\,, .., P_6)$ with $P_j > 0,\, j = 1, 2, .., 6$ is some positive definite matrix.

6.2.6 The closed-loop system

Referring to Eqs. 37–49, the closed-loop system can be written as

$$X' = \begin{bmatrix} 0 & 1 & 0 & 0 & 0 & 0 \\ a_{1\alpha} & a_{2\alpha} & 0 & 0 & 0 & 0 \\ 0 & 0 & 0 & 1 & 0 & 0 \\ 0 & 0 & a_{1\phi} & a_{2\phi} & 0 & a_{3\phi} \\ 0 & 0 & 0 & 0 & 0 & 1 \\ 0 & 0 & 0 & a_{1\gamma} & a_{2\gamma} & a_{3\gamma} \end{bmatrix} \tag{51}$$

where

$$\begin{aligned}
a_{1\alpha} &= -4C(|D_1\, D_2|)_{avg}\, \nu_1 + 3(K_{YX} - K_{ZX}), && (52)\\
a_{2\alpha} &= -4C(|D_1\, D_2|)_{avg}\, \mu_1, && (53)\\
a_{1\phi} &= \frac{1}{K_{ZX}}[-2C(|D_1\, D_2|)_{avg}\, \nu_3 + 4(1 - K_{YX})], && (54)\\
a_{2\phi} &= \frac{1}{K_{ZX}}[-2C(|D_1\, D_2|)_{avg}\, \mu_3], && (55)\\
a_{3\phi} &= -\frac{1}{K_{ZX}}[-1 + K_{YX} + K_{ZX}], && (56)\\
a_{1\gamma} &= -\frac{1}{K_{YX}}[1 - K_{YX} - K_{ZX}], && (57)\\
a_{2\gamma} &= -\frac{1}{K_{YX}}[-D_3\, \nu_2 + (1 - K_{ZX})], && (58)\\
a_{3\gamma} &= \frac{1}{K_{YX}}(-D_3\, \mu_2), && (59)
\end{aligned}$$

Here, the term $|D_1 D_2|_{avg}$ is obtained as follows. First, the term $D_1 D_2$ can be expressed using Eqs. 43 and 44 as

$$D_1 D_2 = E\, sin(2\theta + \varphi) \tag{60}$$

where

$$\begin{aligned}
E &= \sqrt{E_1^2 + E_2^2} \\
E_1 &= \frac{1}{2}[cos^2\, \psi - sin^2\, \psi\, cos^2\, (i - \epsilon_s)] \\
E_2 &= -cos\, \psi\, sin\, \psi\, cos\, (i - \epsilon_s) \\
\varphi &= tan^{-1}\left(\frac{E_2}{E_1}\right)
\end{aligned}$$

The average value of the term D_1D_2 is

$$|D_1D_2|_{avg} = \frac{2}{\pi}\int_{-\frac{\varphi}{2}}^{\frac{(\pi-\varphi)}{2}} E\,sin(2\theta+\varphi)\,d\theta = \frac{2E}{\pi} \tag{61}$$

Using Eqs. 50–51 and applying the condition of asymptotical stability of the system given by $V' < 0$ yield

$$\mu_j > 0,\ j = 1,2,3 \tag{62}$$

$$\nu_1 > \frac{3(K_2-K_1)}{4C\,|D_1D_2|_{avg}(1-K_1K_2)} \tag{63}$$

$$\nu_2 > \frac{K_2(1-K_1)}{(1-K_1K_2)D_3} \tag{64}$$

$$\nu_3 > \frac{2K_1(1-K_2)}{C\,|D_1D_2|_{avg}(1-K_1K_2)} \tag{65}$$

Note in the preceding Eqs. 63-65, K_{YX} and K_{ZX} are replaced by K_1 and K_2 using the relations $K_{YX} = (1-K_1)/(1-K_1K_2)$ and $K_{ZX} = (1-K_2)/(1-K_1K_2)$.

7 Next simple criteria

7.1 Objective

To find the satellite in the Earth shadow as the proposed control strategy would become ineffective whenever the satellite is in the Earth shadow.

7.1.1 Assumptions

1. Assuming the Earth a perfect sphere.
2. The Sun at an infinite distance from the Earth.

7.2 the conditions for the satellite to be in the Earth's shadow

$$cos\,\xi < 0 \quad \& \quad R_E - R\sqrt{(1-cos^2\,\xi)} > 0 \tag{66}$$

where

$$cos\,\xi = cos\,\psi\,cos\,\theta + sin\,\psi\,sin\,\theta\,cos\,(i-\epsilon_s), \tag{67}$$

$$R = R_a\left(\frac{1-e^2}{1+e\,cos\,\theta}\right). \tag{68}$$

8 Numerical Simulation

n order to study the performance of the proposed control strategy, the detailed system response is numerically simulated using Eqs, 8–10 and 20–22 with a generic satellite model

of inertia matrix:

$$\boldsymbol{I}_s = \begin{pmatrix} 200 & 0 & 0 \\ 0 & 150 & 0 \\ 0 & 0 & 175 \end{pmatrix} kg\, m^2 \tag{69}$$

and the parameters given in Table 1.

The integration is carried out using the International Mathematical and Statistical Library (IMSL) routine DDASPG based on the Petzoid-Gear BDF method. The Earth shadow effect is assumed as per Eqs. 66- 68. The control laws as per Eqs. 47–49 are applied along with the restrictions on solar flap rotation angles and the maximum magnetic moment (taking $N_c = 100$, $I_c = 0.5\, A$, $A_c = 0.25\, m^2$) as

$$|\beta_j|_{max} = 40^\circ,\ |\eta_j|_{max} = 40^\circ,\ |\vec{M}|_{max} = 12.5\, A\, m^2 \tag{70}$$

These numerical values were taken considering the practical feasibility of the proposed controller. The control gains in Eqs. 47–49 are selected, as tabulated in Table 1, based on the asymptotic stability conditions, Eqs. 62 - 65 and desired system response. Note the external disturbance torques acting on the satellite are only gravity-gradient torques as given in Eq. 23.

Table 1
System parameters and initial conditions for numerical simulation

$GM_E = 3.986 \times 10^{14}\,m^3/s^2$, $p = 4.563 \times 10^{-6}\,N/m^2$,
$R_a = 42{,}241$ km, $\varepsilon_s = 23.5^\circ$, $i = 0^\circ$, $\alpha_d = \phi_d = \gamma_d = 0$,
$\alpha_0 = \phi_0 = 20^\circ$, $\gamma_0 = 5^\circ$, $\alpha_0' = \phi_0' = \gamma_0' = 0.1$
Solar flap parameters: $A_1 = 1\,m^2$, $r_1 = 2$ m, $\rho_s = 0.7$, $\rho_d = 0$
Control gains: $\mu_1 = 2.5$, $\nu_1 = 5$, $\mu_2 = 0.05$, $\nu_2 = 0.2$, $\mu_3 = 0.3$, $\nu_3 = 0.5$

9 Results and Discussion

First the case when the satellite is orbiting in a circular orbit (i.e., $e \approx 0$) is considered.

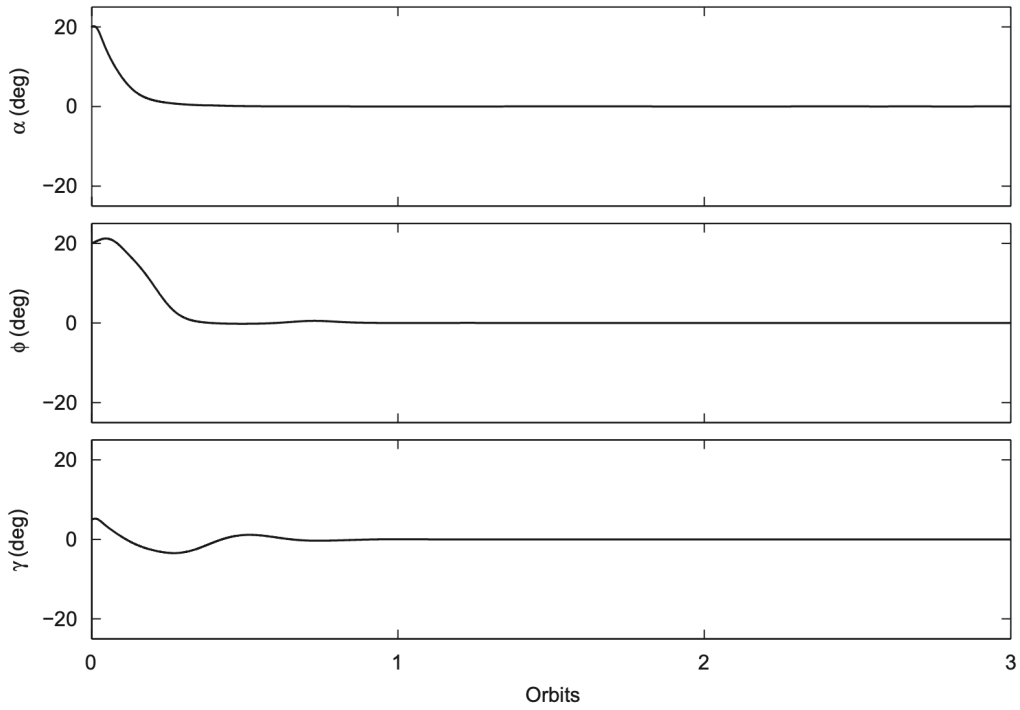

Fig. 2. Satellite attitude response: $e = 0$, $\psi = 45^\circ$, $\Delta d = 0$.

Fig. 2 shows the satellite attitude response in the presence of initial attitude disturbances. The proposed controller is successful in stabilizing the satellite in less than half an orbit and the attitude angles reach to almost zero (see Table 2).

Table 2
Maximum steady-state attitude angles for response plots

Figure	Attitude angles (in two orbits)
2	$\|\alpha\|_{\max} = 1.49 \times 10^{-5\circ}$, $\|\phi\|_{\max} = 4.11 \times 10^{-5\circ}$, and $\|\gamma\|_{\max} = 7.46 \times 10^{-5\circ}$
4	$\psi = 90^\circ$: $\|\alpha\|_{\max} = 5.59 \times 10^{-5\circ}$, $\|\phi\|_{\max} = 4.08 \times 10^{-4\circ}$, $\|\gamma\|_{\max} = 2.64 \times 10^{-4\circ}$
	$\psi = 135^\circ$: $\|\alpha\|_{\max} = 4.55 \times 10^{-6\circ}$, $\|\phi\|_{\max} = 1.43 \times 10^{-4\circ}$, $\|\gamma\|_{\max} = 9.45 \times 10^{-5\circ}$
	$\psi = 180^\circ$: $\|\alpha\|_{\max} = 2.58 \times 10^{-9\circ}$, $\|\phi\|_{\max} = 9.92 \times 10^{-5\circ}$, $\|\gamma\|_{\max} = 9.59 \times 10^{-5\circ}$
6	$e = 0.001$: $\|\alpha\|_{\max} = 0.003^\circ$, $\|\phi\|_{\max} = 0.002^\circ$, and $\|\gamma\|_{\max} = 0.001^\circ$
	$e = 0.1$: $\|\alpha\|_{\max} = 0.417^\circ$, $\|\phi\|_{\max} = 0.159^\circ$, and $\|\gamma\|_{\max} = 0.065^\circ$
7	Case (c): $\|\alpha\|_{\max} = 3.7 \times 10^{-2\circ}$, $\|\phi\|_{\max} = 7.31 \times 10^{-2\circ}$, and $\|\gamma\|_{\max} = 0.14^\circ$
8	$\Delta d = 0.001$: $\|\alpha\|_{\max} = 2.41 \times 10^{-2\circ}$, $\|\phi\|_{\max} = 2.76 \times 10^{-3\circ}$, and $\|\gamma\|_{\max} = 4.33 \times 10^{-4\circ}$
	$\Delta d = 0.01$:$\|\alpha\|_{\max} = 0.24^\circ$, $\|\phi\|_{\max} = 2.78 \times 10^{-2\circ}$, and $\|\gamma\|_{\max} = 3.78 \times 10^{-3\circ}$
9	$\psi = 180^\circ$: $\|\alpha\|_{\max} = 0.29^\circ$, $\|\phi\|_{\max} = 6.61 \times 10^{-2\circ}$, and $\|\gamma\|_{\max} = 0.14^\circ$

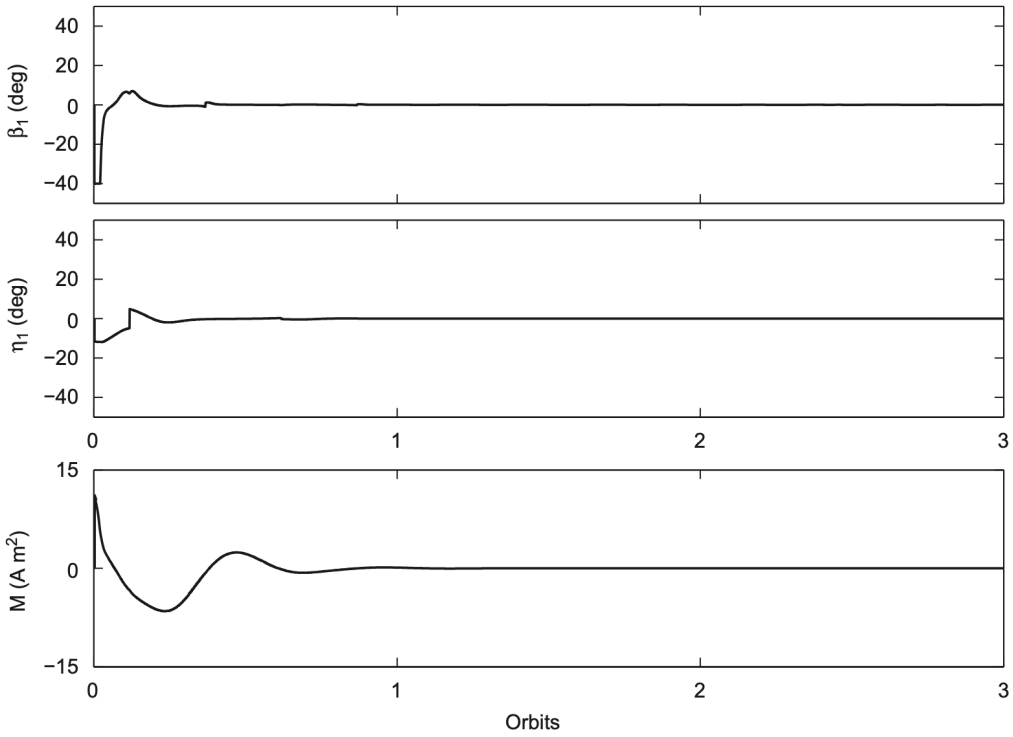

Fig. 3. Control input history: $e = 0$, $\psi = 45^\circ$, $\Delta d = 0$.

The corresponding controller response is shown in Fig. 3. The solar flap rotation angles, β_1 and η_1, as well as the magnetic moment, M, all are within the permissible limits as per Eqs. 70. In Fig. 3, only the β_1 and η_1 responses are shown while the β_2 and η_2 responses as per Eqs. 47 and 48 are just opposite to that of the β_1 and η_1 responses.

Note that the initial yaw attitude error is considered smaller than the pitch and roll attitude errors. This is because the magnetic torque at the geostationary altitude is rather low and with the restrictions as per Eqs. 70, the torque available to control the yaw motion is smaller than the torque for controlling pitch and roll motions. In real situations, the limit on the yaw error is, in general, higher than the pitch and roll errors and therefore, even with the small yaw torque available, it is possible to achieve the desired attitude performance as shown in Fig. 2.

In the simulation (Figs.2 and 3), the magnetic field strength is taken as a constant. However, during high solar activity, it varies in amplitude as much as ± 40 percent and on very rare occasions during severe solar activity, temporary reversal of the field occurs.

The system response remains virtually unaffected (as shown in Figs. 2 and 3) in the case the magnetic field strength dropped by 50 percent of the nominal value.

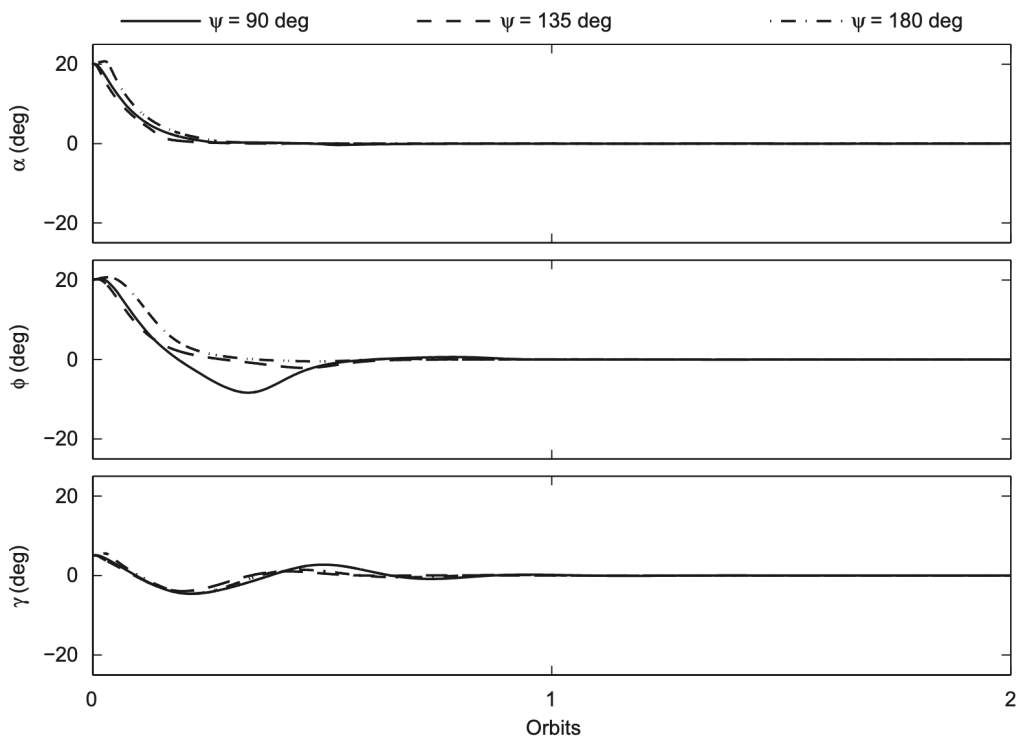

Fig. 4. Effect of sun angle ψ on satellite attitude response: $e = 0$, $\Delta d = 0$.

Next the effect of the solar angle ψ on the controller performance is examined (Fig. 4). As ψ is changed from 90° to 180°, the satellite attitude response remains almost unaffected with its attitude stabilizing in half an orbit. However, the satellite attitude response remains virtually unaffected (see Table 2).

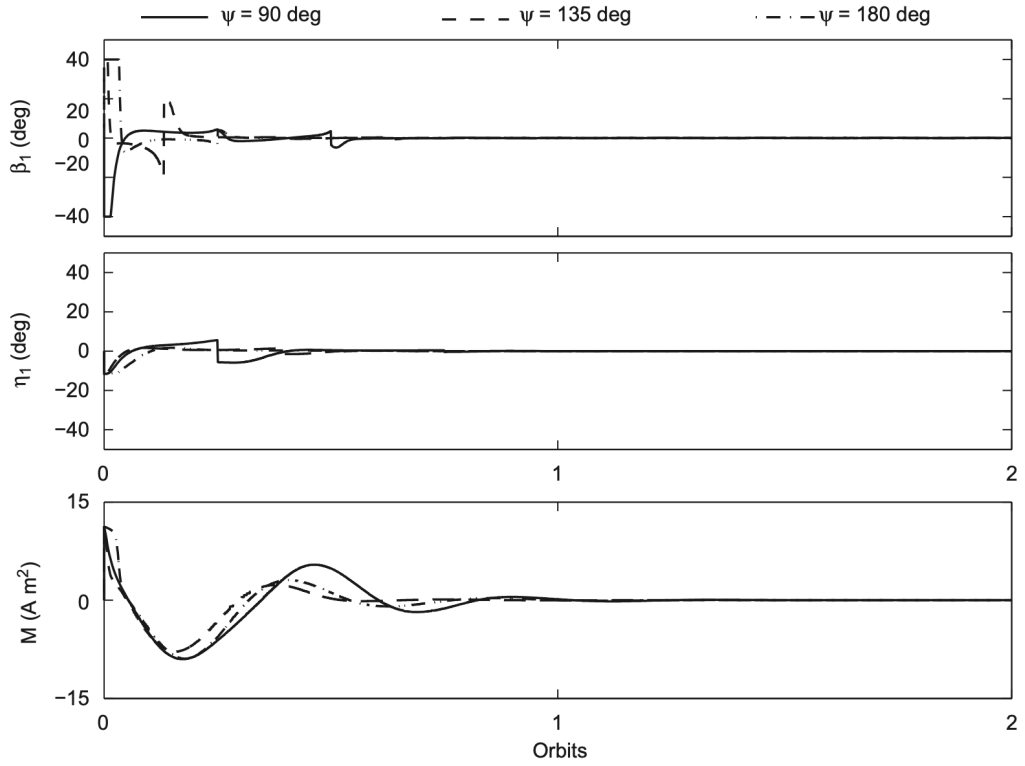

Fig. 5. Control input history: $e = 0$, $\Delta d = 0$.

The effect of orbital eccentricity on the satellite attitude response is next studied (Fig. 6). As orbital eccentricity is increased from $e \approx 0.001$ to 0.1, the attitude angles vary as shown in Table 2. The system pitch equation of motion, Eq. 30 is linearized by considering small amplitude librations and low eccentricities, and ignoring the second and higher order terms in α and e. Using solar pitch torque Eq. 45 and control law Eq. 47, the resulting pitch equation of motion is

$$\alpha'' + 4C\,|D_1|\,|D_2|\,\mu_1\,\alpha' + [-3(K_Y X - K_Z X) + 4C\,|D_1|\,|D_2|\,\nu_1]\alpha = 2\,e\,sin\,\theta \tag{71}$$

Taking the average value of the term $D_1 D_2$ given by Eq. 61 and substituting it into Eq. 71, the solution of pitch motion is obtained as

$$\alpha = A_1 e^{s_1\,\theta} + A_2 e^{s_2\,\theta} + A_3\,sin\,\theta + A_4\,cos\,\theta \tag{72}$$

where

$$s_1 = \frac{-a - \sqrt{a^2 - 4b}}{2} \tag{73}$$

$$s_2 = \frac{-a + \sqrt{a^2 - 4b}}{2} \tag{74}$$

$$a = \frac{8CE\mu_1}{\pi} \tag{75}$$

$$b = -3(K_{YX} - K_{ZX}) + \frac{8CE\nu_1}{\pi} \tag{76}$$

$$c = 2e \tag{77}$$

$$A_1 = \frac{s_2\,\alpha_0 + \alpha_0' - A_3 - A_4 s(1 + s_1)}{s_2 - s_1} \tag{78}$$

$$A_2 = \frac{-s_1\,\alpha_0 + \alpha_0' - A_3 - A_4 s}{s_2 - s_1} \tag{79}$$

$$A_3 = \frac{c(b-1)}{[a^2 + (b-1)^2]} \tag{80}$$

$$A_4 = \frac{ca}{[a^2 + (b-1)^2]} \tag{81}$$

$$\tag{82}$$

From Eq. 72, the first two terms correspond to transient response while the last two terms correspond to steady-state response.

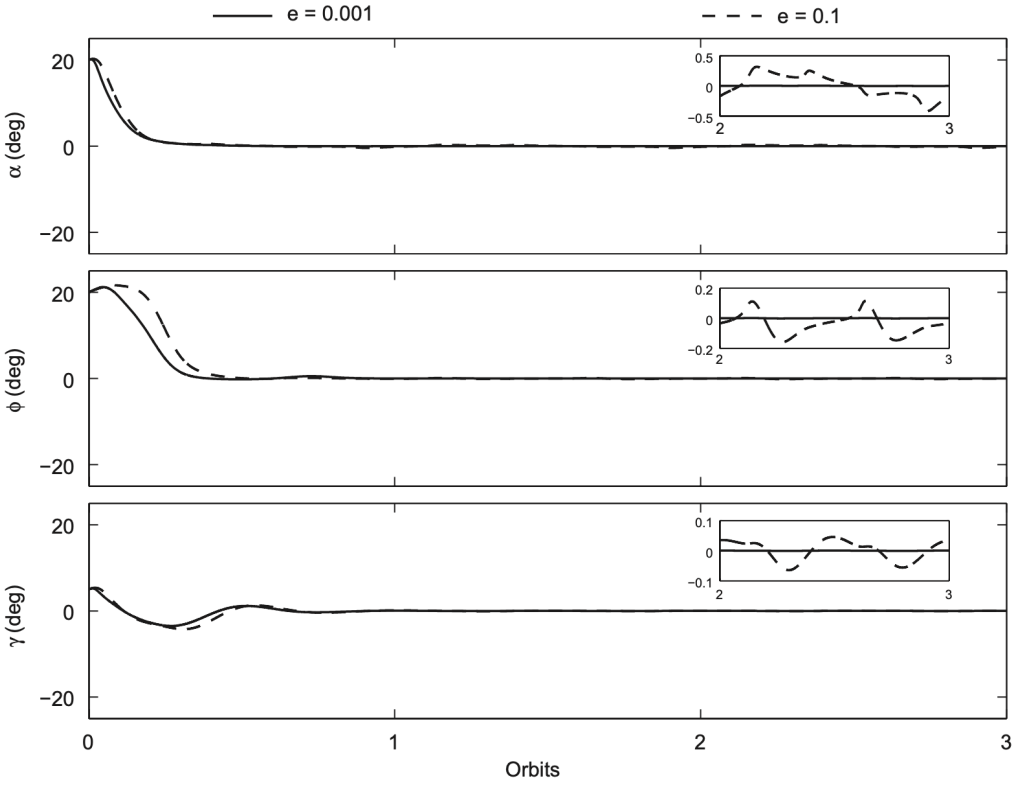

Fig. 6. Satellite attitude response as affected by orbital eccentricity: $\psi = 45°$, $\Delta d = 0$.

This analytical solution matches with the numerical solution shown in Fig. 6.

For the case of orbital eccentricity $e \approx 0.1$, the satellite attitude response remains stable with small attitude errors as expected from Eq. 72.

Next, the effect of changes in satellite mass inertia matrix, Is on the controller performance is examined (Fig. 7). Three cases are taken

$$\boldsymbol{I}_s = \begin{pmatrix} 200 & 0 & 0 \\ 0 & 150 & 0 \\ 0 & 0 & 175 \end{pmatrix} kg\, m^2 \tag{83}$$

$$\boldsymbol{I}_s = \begin{pmatrix} 175 & 0 & 0 \\ 0 & 200 & 0 \\ 0 & 0 & 175 \end{pmatrix} kg\, m^2 \tag{84}$$

$$\boldsymbol{I}_s = \begin{pmatrix} 190 & -0.95 & -1.71 \\ -0.95 & 180 & 1.14 \\ -1.71 & 1.14 & 150 \end{pmatrix} kg\, m^2 \tag{85}$$

Note that the second and third cases correspond to an unstable gravity gradient configuration. The proposed controller is able to stabilize the satellite for all the cases considered. However, for the cases (a) and (b), the satellite attitude angles settle to zero while for the case (c), the attitude angles are nonzero (see Table 2).

The corresponding control inputs also remain nonzero with steady state $|\beta_1|_{max} = 0.43^\circ$, $|\eta_1|_{max} = 0.06^\circ$, and $|M|_{max} = 0.25\, A\, m^2$.

Thus, the products of inertia have an adverse effect on the satellite attitude response. In the case higher products of inertia terms are considered, the attitude angles increase and with further increase in the products of inertia the satellite attitude may become unstable as expected with the constant control gains.

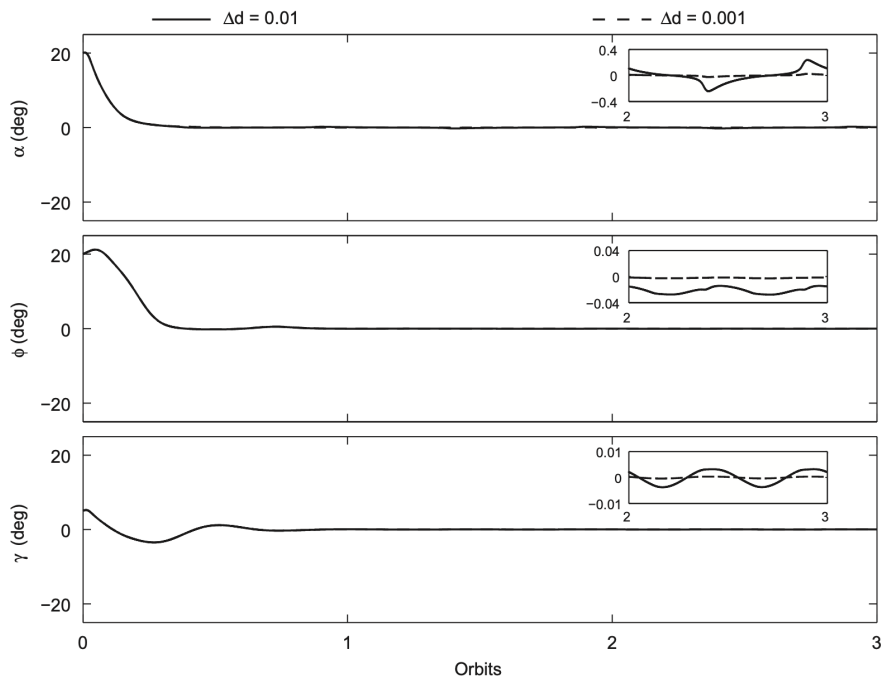

Fig. 8. Effect of the system parameter Δd on satellite attitude response: $e = 0$, $\psi = 45°$, $\Delta d = 0$.

Fig. 8 shows the effect of the system parameter Δd on the satellite attitude response. If Δd is increased from $\Delta d = 0.001$ to 0.01, the satellite attitude response deteriorates (see Table 2). However, the satellite attitude remains stable even for $\Delta d = 0.01$ with attitude errors within a fraction of a degree. It is to be noted that the pitch and roll attitudes are adversely affected while the yaw attitude remained virtually unaffected with changes in Δd. In fact, referring to the SRP torque Eqs. 8–10, the parameter Δd only affects pitch and roll torques and therefore, the yaw attitude remains unaffected. It is important to mention that if Δd is higher that 0.01, the attitude response further deteriorates as expected.

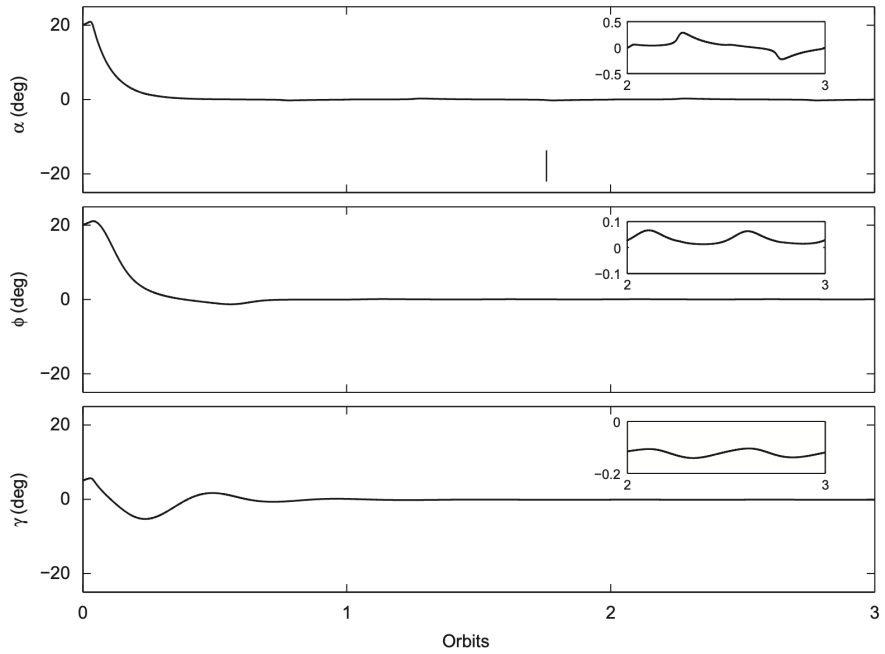

Fig. 9. Satellite attitude response as affected by variations in system parameters: $e = 0.001$, $\psi = 180^\circ$, $\Delta d = 0.01$; $I_{xx} = 190$, $I_{yy} = 180$, $I_{zz} = 150$, $I_{xy} = 0.95$, $I_{yz} = -1.14$, $I_{xz} = 1.71$ (kg m^2).

Finally, a case where all uncertainties considered above are taken together is examined (Fig. 9).

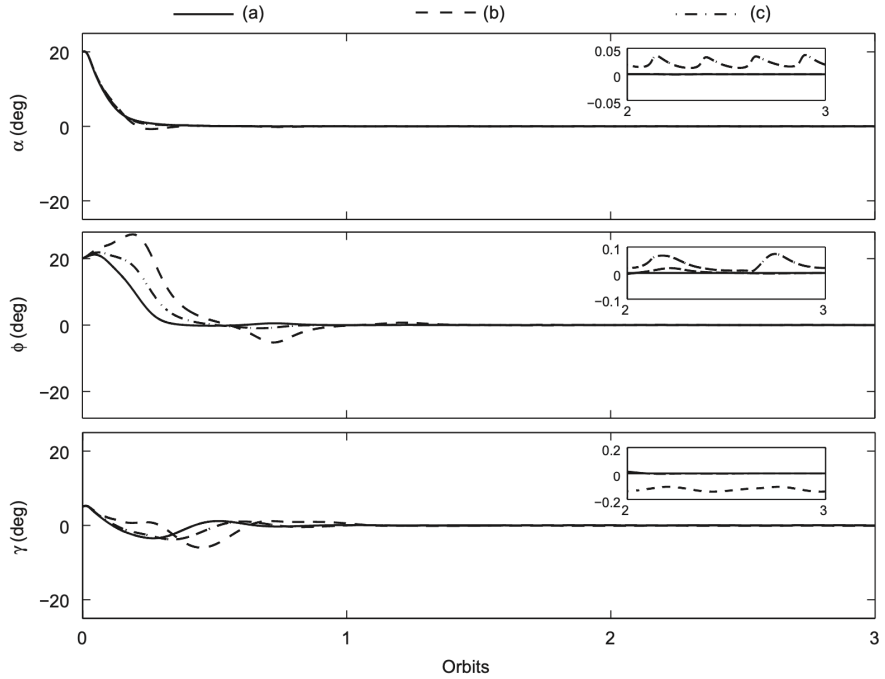

Fig. 7. Satellite attitude response as affected by changes in satellite inertia matrix: $e = 0$, $\psi = 45^\circ$, $\Delta d = 0$: (a) $I_{xx} = 200$, $I_{yy} = 150$, $I_{zz} = 175$ (kg m^2); (b) $I_{xx} = 175$, $I_{yy} = 200$, $I_{zz} = 150$ (kg m^2); and (c) $I_{xx} = 190$, $I_{yy} = 180$, $I_{zz} = 150$, $I_{xy} = 0.95$, $I_{yz} = -1.14$, $I_{xz} = 1.71$ (kg m^2).

The orbital eccentricity, the adverse inertia matrix of case (c) in Fig. 7, and the nonzero Δd are considered along with the adverse solar angle $\psi = 180^\circ$. It is found that even for this adverse situation, the satellite attitude remains stable with attitude errors within a

fraction of a degree (see Table 2). The control inputs are within the permissible limits (i.e., $|\beta_1|_{max} = 3.76°$, $|\eta_1|_{max} = 0.03°$, and $|M|_{max} = 0.25\, A\, m^2$).

Thus, the proposed controller was successful in stabilizing the satellite attitude in the presence of system uncertainties and orbital eccentricity.

10 Conclusions

- The attitude stabilization of a geosynchronous satellite using the SRP torque and magnetorquer is presented.
- The research solves the passive method challenges leading to the practical application of the technology and to achieve the goal of low cost ACSs.
- The efficacy of the controller performance is tested on the nonlinear system model considering various uncertainties in the system parameters including satellite inertia matrix, solar flaps, and orbital eccentricity.
- Results of the numerical simulations indicate that the proposed concept is feasible.
- The SRP torque was successful in controlling the satellite pitch and roll attitudes while the yaw attitude was stabilized by the magnetotorquer.
- The products of inertia, the parameter Δd, the orbital eccentricity, and the magnetic field strength can significantly deteriorate the satellite attitude response.
- However, for moderate uncertainties in these parameters the satellite attitude was stabilized within half an orbit and it remained within a fraction of a degree.
- The control inputs were within the limits of the maximum solar flaps rotation of 40° and with the maximum magnetic rod magnetic moment of 12 A m^2.
- The proposed control strategy can be augmented with the existing attitude control system of the satellite and may extend the life of the satellite mission experiencing attitude actuator failures.
- In the future work, the present study will be extended to include high fidelity Earth's magnetic field and SRP models (that consider Earth rotation, orbit precession, variations in the solar irradiance, and other associated factors), and orbit and attitude coupling for practical realization of the proposed concept.

11 References

[1]. Satellite attitude stabilization using solar radiation pressure and magnetotorquer - by K.D. Kumar, M.J. Tahk, and H.C. Bang